One-loop Wilson loops and the particle-interface potential in AdS/dCFT

de Leeuw, Marius; Ipsen, Asger C.; Kristjansen, Charlotte; Wilhelm, Matthias

Published in:
Physics Letters B

DOI:
10.1016/j.physletb.2017.02.047

Publication date:
2017

Document version
Publisher's PDF, also known as Version of record

Physics Letters B 768 (2017) 192–197

Contents lists available at ScienceDirect

Physics Letters B

www.elsevier.com/locate/physletb

One-loop Wilson loops and the particle-interface potential in AdS/dCFT

Marius de Leeuw, Asger C. Ipsen, Charlotte Kristjansen, Matthias Wilhelm *

Niels Bohr Institute, Copenhagen University, Blegdamsvej 17, 2100 Copenhagen Ø, Denmark

ARTICLE INFO

Article history:
Received 24 November 2016
Received in revised form 17 February 2017
Accepted 19 February 2017
Available online 28 February 2017
Editor: N. Lambert

Keywords:
Holography
AdS/CFT correspondence
D5-D3 system
Wilson loop
Particle-interface potential

ABSTRACT

We initiate the calculation of quantum corrections to Wilson loops in a class of four-dimensional defect conformal field theories with vacuum expectation values based on $\mathcal{N}=4$ super Yang–Mills theory. Concretely, we consider an infinite straight Wilson line, obtaining explicit results for the one-loop correction to its expectation value in the large-N limit. This allows us to extract the particle-interface potential of the theory. In a further double-scaling limit, we compare our results to those of a previous calculation in the dual string-theory set-up consisting of a D5-D3 probe-brane system with flux, and we find perfect agreement.

1. Introduction

Wilson loops form an important class of observables in any gauge theory. Among others, they are related to scattering amplitudes [1] and can be used to determine the quark–antiquark potential [2]. In gauge theories that interact with a boundary or interface, a further important potential is the particle-interface potential, which can likewise be obtained from a Wilson loop. A simple set-up to study this potential is given by defect conformal field theories (dCFTs).

We will be interested in dCFTs with holographic duals, of which a number of examples exist, building on the Karch–Randall idea [3]. More precisely, we will consider $\mathcal{N}=4$ supersymmetric Yang–Mills theory ($\mathcal{N}=4$ SYM theory) with a codimension-one defect at $x_3=0$ separating two regions of space–time where the gauge group is SU(N) and SU($N-k$), respectively [4–7]. To achieve the difference in the rank of the gauge group, a non-vanishing vacuum expectation value (vev) proportional to $1/x_3$ is assigned to three of the scalar fields in the region $x_3>0$. The resulting gauge theory is dual to a D5-D3 probe-brane system involving a single D5 brane of geometry $AdS_4\times S^2$ supporting a background gauge field flux of k units through the S^2.

A special feature of dCFTs is that one-point functions of gauge-invariant local composite operators can be non-vanishing [8]. One-point functions of the present dCFT were studied at tree level in [9–13]. Furthermore, in [14] we set up the program for performing perturbative calculations in the dCFT and treated one-point functions as the first simple application. This opened the possibility of performing more elaborate comparisons between gauge- and string-theory results in a certain double-scaling limit, which is imposed on top of the planar limit by taking the 't Hooft coupling $\lambda\to\infty$ and $k\to\infty$ while keeping λ/k^2 finite, as proposed in [9,15].

In this letter, we initiate the calculation of quantum corrections to non-local observables in the dCFT under consideration. Concretely, we calculate the one-loop correction of a particular Wilson loop in the large-N limit which allows us to extract the corresponding correction to the particle-interface potential. This Wilson loop was already considered at tree level in [15], where also the corresponding string-theory calculation was performed. After giving a brief introduction to the dCFT in section 2, we describe our calculation of the Wilson loop in section 3. This calculation builds heavily on [14], and we refer the reader to this reference and to the forthcoming article [16] for details. In section 4, we then compare our planar result to the string-theory result of [15] in the aforementioned double-scaling limit, finding perfect agreement exactly as for one-point functions [14]. Finally, section 5 contains our conclusion and outlook.

* Corresponding author.
E-mail addresses: deleeuwm@nbi.ku.dk (M. de Leeuw), asgercro@nbi.ku.dk (A.C. Ipsen), kristjan@nbi.ku.dk (C. Kristjansen), matthias.wilhelm@nbi.ku.dk (M. Wilhelm).

http://dx.doi.org/10.1016/j.physletb.2017.02.047

2. The defect theory

The action of the dCFT is given by the action of the four-dimensional $\mathcal{N}=4$ SYM theory plus an action describing a three-dimensional fundamental hypermultiplet on the defect as well as its coupling to the bulk fields [4–7]. We use the following form of the action of $\mathcal{N}=4$ SYM theory

$$S_{\mathcal{N}=4} = \frac{2}{g_{\rm YM}^2}\int \mathrm{d}^4x\,\mathrm{tr}\left(-\frac{1}{4}F_{\mu\nu}F^{\mu\nu} - \frac{1}{2}\,\mathrm{D}_\mu\phi_i\,\mathrm{D}^\mu\phi_i + \frac{i}{2}\bar\psi\Gamma^\mu\,\mathrm{D}_\mu\psi + \frac{1}{2}\bar\psi\Gamma^i[\phi_i,\psi] + \frac{1}{4}[\phi_i,\phi_j][\phi_i,\phi_j]\right); \tag{1}$$

see [14,16] for details on our conventions. As in the case of one-point functions, the three-dimensional action will not play any role in the present one-loop calculation; the reason is that the only potentially contributing Feynman diagram would involve a loop consisting of a single propagator of a defect field which vanishes due to conformal invariance.[1]

Of the different fields in $\mathcal{N}=4$ SYM theory, three scalars acquire a non-vanishing vev encoding the so-called fuzzy-funnel solution [7]:

$$\langle\phi_i\rangle_{\rm tree} = \phi_i^{\rm cl} = -\frac{1}{x_3}t_i \oplus 0_{(N-k)\times(N-k)}\,, \qquad x_3>0\,, \tag{2}$$

where $i=1,2,3$. Here, t_1, t_2 and t_3 are the generators of the k-dimensional irreducible representation of the SU(2) Lie algebra. In particular, t_3 is a diagonal matrix with eigenvalues

$$d_{k,i} = \frac{1}{2}(k-2i+1)\,, \qquad i=1,\ldots,k\,. \tag{3}$$

In order to calculate quantum corrections, we expand the action (1) around the classical solution, writing

$$\phi_i = \phi_i^{\rm cl} + \tilde\phi_i\,, \qquad i=1,2,3\,. \tag{4}$$

The explicit form of the (gauge-fixed) action resulting from this is given in [14,16]. In contrast to the usual action (1) of $\mathcal{N}=4$ SYM theory, this action contains a quadratic mass-like term, which moreover has two non-standard properties.

The first non-standard property of the mass-like term is that it is non-diagonal in the colour components of the different fields. This is caused by the classical solution (2) taking values in the k-dimensional representation of the Lie algebra SU(2) in colour space. Moreover, also some of the flavours mix, concretely the scalars $\tilde\phi_1$, $\tilde\phi_2$ and $\tilde\phi_3$ with the component A_3 of the gauge field and the fermion flavours among each other. This mixing problem was solved in [14,16]. The eigenvalues are given in Table 1, partially in terms of

$$\nu = \sqrt{m^2+\frac{1}{4}}\,. \tag{5}$$

The second non-standard property of the mass-like terms is that they depend on $1/x_3$, the inverse distance to the defect. This x_3-dependence in the mass terms can be exchanged for standard mass terms in AdS_4 [14,15], which amounts to performing a Weyl transformation. The scalar propagator resulting from this Weyl transformation can be extracted from the AdS_4 propagator given e.g. in [17]:

$$K(x,y) = \frac{g_{\rm YM}^2\sqrt{x_3y_3}}{2}\int\frac{\mathrm{d}^3\vec k}{(2\pi)^3}\,\mathrm{e}^{i\vec k\cdot(\vec x-\vec y)}\,I_\nu(|\vec k|x_3^<)K_\nu(|\vec k|x_3^>)\,, \tag{6}$$

[1] Defect fields can come into play at higher loop orders.

Table 1
Masses and multiplicities of the different quantum fields, partially given in terms of ν defined in (5) [14]. The ghost field c arises from the gauge fixing. Note that we have suppressed the x_3-dependence for ease of presentation.[2]

Multiplicity	$\nu(\tilde\phi_{4,5,6}, A_{0,1,2}, c)$	$m(\psi_{1,2,3,4})$	$\nu(\tilde\phi_{1,2,3}, A_3)$
$\ell=1,\ldots,k-1$	$\ell+\frac{1}{2}$	$\ell+1$	$\ell+\frac{3}{2}$
$\ell+1$	$\ell+\frac{1}{2}$	$-\ell$	$\ell-\frac{1}{2}$
$(k-1)(N-k)$	$\frac{k}{2}$	$\frac{k+1}{2}$	$\frac{k+2}{2}$
$(k+1)(N-k)$	$\frac{k}{2}$	$-\frac{k-1}{2}$	$\frac{k-2}{2}$
$(N-k)(N-k)$	$\frac{1}{2}$	0	$\frac{1}{2}$

where I_ν and K_ν are modified Bessel functions and $x_3^<$ ($x_3^>$) is the smaller (larger) of x_3 and y_3. Moreover, $\vec k=(k_0,k_1,k_2)$ pertains to the directions parallel to the defect. The fermion propagator can be extracted in a similar way but is not explicitly needed here.

3. Wilson loop

We now calculate the planar one-loop correction to a particular Wilson loop. The colour and flavour parts of the required calculations are very similar to those appearing in the calculation of one-point functions, and we refer the reader to [14,16] for details. The main difference lays in the space–time part.

Set-up Following [15], we consider a straight Wilson line parallel to the defect, which we can parametrise using $\gamma(\alpha)=\alpha n+(0,0,0,x_3)$ with n being a unit vector with $n_3=0$. Without loss of generality, we take $n=(1,0,0,0)$. Let

$$U(\alpha,\beta) = P\exp\int_\alpha^\beta \mathrm{d}t\mathcal{A}(t) \;\text{ with }\; \mathcal{A} = iA_0 - \sin\chi\,\phi_3 - \cos\chi\,\phi_6 \tag{7}$$

be the parallel propagator along this line, where we have abbreviated $U(\alpha,\beta)\equiv U(\gamma(\alpha),\gamma(\beta))$, etc. We then close the open colour indices and define

$$W = \mathrm{tr}\,U(-\tfrac{T}{2},+\tfrac{T}{2})\,. \tag{8}$$

In the limit $T\to\infty$, this yields an infinite straight Wilson line. We depict the classical Wilson line along with its one-loop corrections in Fig. 1.

Expanding the field $\mathcal{A}$ as

$$\mathcal{A} = \mathcal{A}^{\rm cl} + \tilde{\mathcal{A}}\,, \tag{9}$$

the parallel propagator becomes

$$\begin{aligned} U(-\tfrac{T}{2},+\tfrac{T}{2}) &= U^{\rm cl}(-\tfrac{T}{2},+\tfrac{T}{2}) \\ &+ \int_{-\frac{T}{2}}^{+\frac{T}{2}}\mathrm{d}\alpha\,U^{\rm cl}(-\tfrac{T}{2},\alpha)\tilde{\mathcal{A}}(\alpha)U^{\rm cl}(\alpha,+\tfrac{T}{2}) \\ &+ \int_{-\frac{T}{2}}^{+\frac{T}{2}}\mathrm{d}\alpha\int_\alpha^{+\frac{T}{2}}\mathrm{d}\beta\,U^{\rm cl}(-\tfrac{T}{2},\alpha)\tilde{\mathcal{A}}(\alpha)U^{\rm cl}(\alpha,\beta)\tilde{\mathcal{A}}(\beta)U^{\rm cl}(\beta,+\tfrac{T}{2}) \\ &+ \text{higher orders in the quantum fields}\,, \end{aligned} \tag{10}$$

[2] Note that the negative signs of the fermion masses can be absorbed into a chiral rotation of the fermions, cf. [14].

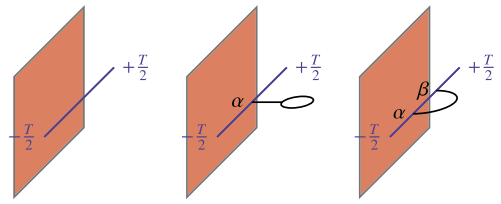

Fig. 1. Tree-level (a) and one-loop ((b) lollipop and (c) tadpole) contributions to the expectation value of the Wilson line. The defect is drawn in red, the classical Wilson line in blue and propagators in black. (For interpretation of the references to colour in this figure legend, the reader is referred to the web version of this article.)

where $U^{\rm cl}$ denotes U with $\mathcal{A}$ replaced by the classical field $\mathcal{A}^{\rm cl}$ and the higher orders in the quantum fields start to contribute only at two-loop order.

Tree level At tree level, we have [15]

$$\begin{aligned}\langle W\rangle_{\rm tree} &= \operatorname{tr} U^{\rm cl}(-\tfrac{T}{2},+\tfrac{T}{2}) = \operatorname{tr}\exp\left(-T\sin\chi\,\phi_3^{\rm cl}\right)\\ &= (N-k)+\sum_{i=1}^{k}\exp\left(T\frac{\sin\chi}{x_3}d_{k,i}\right)\\ &= (N-k)+\mathrm{e}^{-\frac{1}{2}(k-1)\frac{\sin\chi}{x_3}T}\,\frac{1-\mathrm{e}^{k\frac{\sin\chi}{x_3}T}}{1-\mathrm{e}^{\frac{\sin\chi}{x_3}T}}\\ &\overset{T\to\infty}{\simeq} \mathrm{e}^{\frac{1}{2}(k-1)\frac{\sin\chi}{x_3}T},\end{aligned} \tag{11}$$

where we have used that the only non-vanishing classical field in $\mathcal{A}$ is ϕ_3, which is diagonal with eigenvalues given in (3).

One loop At one-loop order, only two different diagrams contribute – and both of them have direct counterparts in the calculation of one-point functions performed in [14]. The first diagram was called the lollipop diagram in [14] and is depicted in Fig. 1(b), while the second diagram was called the tadpole diagram in [14] and is depicted in Fig. 1(c). Although the second diagram no longer looks like a tadpole, we nevertheless keep the name.

Lollipop diagram The lollipop contribution stems from the second line in (10), where the quantum field is connected by a propagator to a cubic vertex in the action, whose other two fields are also connected by a propagator. We find

$$\begin{aligned}\langle W\rangle_{\text{1-loop,lol}} &= \left\langle \operatorname{tr}\int_{-\frac{T}{2}}^{-\frac{T}{2}} \mathrm{d}\alpha\, U^{\rm cl}(-\tfrac{T}{2},\alpha)\tilde{\mathcal{A}}(\alpha)U^{\rm cl}(\alpha,+\tfrac{T}{2})\right\rangle\\ &= T\sum_i \exp\left[T\frac{\sin\chi}{x_3}d_{k,i}\right]\left\langle[\tilde{\mathcal{A}}]_{ii}\right\rangle_{\text{1-loop}},\end{aligned} \tag{12}$$

where we have used that the parallel propagator is a diagonal matrix with non-zero entries

$$[U^{\rm cl}(\alpha,\beta)]_{ii} = \exp\left[(\beta-\alpha)\frac{\sin\chi}{x_3}d_{k,i}\right]. \tag{13}$$

In [14,16], we have found that, even at finite N,

$$\langle[\tilde{\mathcal{A}}]_{ii}\rangle_{\text{1-loop}} = 0\,, \tag{14}$$

when using a supersymmetry-preserving renormalisation scheme. Thus, the total lollipop contribution to the Wilson line also vanishes before taking the planar limit:

$$\langle W\rangle_{\text{1-loop,lol}} = 0\,. \tag{15}$$

Tadpole diagram In the tadpole diagram, the two quantum fields in the third line of (10) are connected by a propagator. In the large-N limit, only the identity in either the parallel propagator in between the two quantum fields or in both other parallel propagators contributes. Using (13), we thus find that the planar contribution of the tadpole diagram is

$$\begin{aligned}\langle W\rangle_{\text{1-loop,tad}} = &\int_{-\frac{T}{2}}^{+\frac{T}{2}}\mathrm{d}\alpha\int_{\alpha}^{+\frac{T}{2}}\mathrm{d}\beta\left(\exp\left[-(\alpha-\beta)\frac{\sin\chi}{x_3}d_{k,i}\right]\langle[\tilde{\mathcal{A}}]_{ai}(\alpha)[\tilde{\mathcal{A}}]_{ia}(\beta)\rangle\right.\\ &\left.+\exp\left[(\alpha-\beta+T)\frac{\sin\chi}{x_3}d_{k,i}\right]\langle[\tilde{\mathcal{A}}]_{ia}(\alpha)[\tilde{\mathcal{A}}]_{ai}(\beta)\rangle\right),\end{aligned} \tag{16}$$

where $i=1,\dots,k$ and $a=k+1,\dots,N$ are summed over; note that the contribution of the $(N-k)\times(N-k)$ block vanishes. From [14,16], we know that in the large-N limit

$$\begin{aligned}&\langle[\tilde{\mathcal{A}}]_{ia}(\alpha)[\tilde{\mathcal{A}}]_{aj}(\beta)\rangle = \langle[\tilde{\mathcal{A}}]_{ai}(\alpha)[\tilde{\mathcal{A}}]_{ja}(\beta)\rangle\\ &= -\langle[A_0]_{ia}(\alpha)[A_0]_{aj}(\beta)\rangle + \sin^2\chi\,\langle[\tilde{\phi}_3]_{ia}(\alpha)[\tilde{\phi}_3]_{aj}(\beta)\rangle\\ &\qquad + \cos^2\chi\,\langle[\tilde{\phi}_6]_{ia}(\alpha)[\tilde{\phi}_6]_{aj}(\beta)\rangle\\ &= \delta_{ij}N\sin^2\chi\left(\tfrac{k-1}{2k}K^{m^2=\frac{(k+2)^2-1}{4}}+\tfrac{k+1}{2k}K^{m^2=\frac{(k-2)^2-1}{4}}-K^{m^2=\frac{k^2-1}{4}}\right),\end{aligned} \tag{17}$$

where the occurring propagators (6) only depend on $\delta=\beta-\alpha$ and the distance x_3 to the defect. In particular, let us parameterise $x=(\alpha,0,0,x_3)$, $y=(\beta,0,0,0,x_3)$. Then (6) specialises to

$$K(x_3;\delta) = \frac{g_{\rm YM}^2 x_3}{2}\int\frac{\mathrm{d}^3\vec{k}}{(2\pi)^3}\,\mathrm{e}^{-i\vec{k}\cdot\vec{n}\,\delta}\,I_\nu(|\vec{k}|x_3)K_\nu(|\vec{k}|x_3)\,. \tag{18}$$

In order to perform this integral, we decompose the $\vec{k}$ integration into spherical coordinates:

$$K(x_3;\delta) = \frac{g_{\rm YM}^2 x_3}{8\pi^2}\int_0^\infty\mathrm{d}r\,r^2\int_0^\pi\sin\theta\,\mathrm{d}\theta\,\mathrm{e}^{-ir\delta\cos\theta}\,I_\nu(rx_3)K_\nu(rx_3)\,, \tag{19}$$

where we have already performed the trivial azimuth-angle integral. The θ integration yields

$$K(x_3;\delta) = \frac{g_{\rm YM}^2 x_3}{(2\pi)^2}\int_0^\infty\mathrm{d}r\,r\frac{\sin(\delta r)}{\delta}I_\nu(rx_3)K_\nu(rx_3)\,. \tag{20}$$

Next, let us turn to the α, β integrations in (16). Since all functions in the integral only depend on δ, we make the coordinate transformation $(\alpha,\beta)\to(\delta,\beta)$, for which the integral becomes

$$\int_{-\frac{T}{2}}^{+\frac{T}{2}}\mathrm{d}\alpha\int_{\alpha}^{+\frac{T}{2}}\mathrm{d}\beta\to\int_0^T\mathrm{d}\delta\int_{-\frac{T}{2}+\delta}^{+\frac{T}{2}}\mathrm{d}\beta\,. \tag{21}$$

Since the integrand only depends on δ, we can trivially perform the β integration resulting in a factor of $T-\delta$.

We are interested in the large-T limit, which implies that from the prefactor in (16) only the term with $i=1$ will contribute. For simplicity, let us introduce $\eta=\frac{k-1}{2}\sin\chi$. Moreover, in order to make the x_3-dependence explicit, we rescale $r\to r/x_3$. This then combines into the following integral

$$\langle W\rangle_{\text{1-loop,tad}} = \frac{\sin^2\chi}{x_3}\frac{\lambda}{(2\pi)^2}\int_0^T \mathrm{d}\delta \int_0^\infty \mathrm{d}r$$
$$(T-\delta)\left(\exp\left[\delta\,\eta/x_3\right]+\exp\left[(T-\delta)\,\eta/x_3\right]\right)\frac{\sin(\delta r/x_3)}{\delta} \qquad (22)$$
$$r\left(\frac{k-1}{2k}I_{\frac{k+2}{2}}(r)K_{\frac{k+2}{2}}(r)+\frac{k+1}{2k}I_{\frac{k-2}{2}}(r)K_{\frac{k-2}{2}}(r)-I_{\frac{k}{2}}(r)K_{\frac{k}{2}}(r)\right).$$

We can use partial integration on the Bessel function part including the factor of r. This eliminates the δ^{-1} term. As a result, the δ integral in the large-T limit becomes straightforward. After making use of the Bessel function identities in (A.1), this finally leads us to the following integral:

$$\langle W\rangle_{\text{1-loop,tad}} \overset{T\to\infty}{\simeq} \frac{\sin^2\chi}{x_3}\frac{\lambda}{4\pi^2}T\exp\left[\frac{\eta T}{x_3}\right] \qquad (23)$$
$$\int_0^\infty \mathrm{d}r\,\frac{\eta}{r^2+\eta^2}\left(\frac{1}{2}-r\,I'_{\frac{k}{2}}(r)K_{\frac{k}{2}}(r)-\frac{1}{2}I_{\frac{k}{2}}(r)K_{\frac{k}{2}}(r)\right).$$

The rational part can be easily integrated and we are finally left with

$$\langle W\rangle_{\text{1-loop,tad}} \overset{T\to\infty}{\simeq} \frac{\sin^2\chi}{x_3}\frac{\lambda}{4\pi^2}T\exp\left[\frac{\eta T}{x_3}\right]\left(\frac{\pi}{4}-A\right), \qquad (24)$$

where

$$A=\int_0^\infty \mathrm{d}r\,\frac{\eta}{r^2+\eta^2}\left[r\,I'_{\frac{k}{2}}(r)K_{\frac{k}{2}}(r)+\frac{1}{2}I_{\frac{k}{2}}(r)K_{\frac{k}{2}}(r)\right]. \qquad (25)$$

Odd k For odd values of k, the index on the Bessel functions becomes half-integer. For half-integer values, the Bessel functions I_ν, K_ν are given by finite sums for which the integral (25) can be carried out. The result is[3]

$$A=\frac{\pi}{4}-(\log(2\eta)+\gamma_E)\frac{{}_1F_2\left(\frac{3-k}{2};1-k,\frac{2-k}{2};-\eta^2\right)}{2\eta^k}\frac{\Gamma\left(\frac{k}{2}\right)\Gamma(k)}{\sqrt{\pi}\,\Gamma\left(\frac{k-1}{2}\right)}$$
$$-\left(\frac{i\eta K_{\frac{k-2}{2}}(i\eta)+\frac{k-1}{2}K_{\frac{k}{2}}(i\eta)}{2\pi\,i^k}K_{\frac{k}{2}}(i\eta)(\mathrm{Ei}(2i\eta)-i\pi)+\text{c.c.}\right)$$
$$+\sum_{l=0}^{\lfloor\frac{k+1}{4}\rfloor}\sum_{m=0}^{\frac{k-1}{2}}\sum_{n=1}^{2l+m}\frac{H_n}{(2l)!m!n!}\frac{i^{k-1}(-1)^l}{(2\eta)^{2l+m-n}}\frac{\Gamma\left(\frac{k+1}{2}+2l\right)\Gamma\left(\frac{k+1}{2}+m\right)}{\Gamma\left(\frac{k+1}{2}-2l\right)\Gamma\left(\frac{k+1}{2}-m\right)}$$
$$\times\left[\frac{[k^2+(4l-1)^2-2]\sin\frac{\pi(m+n)}{2}}{4(4l+k-1)(4l-k-1)}\right.$$
$$\left.-\frac{[k^2+(4l+1)^2-2]\cos\frac{\pi(m+n)}{2}}{32(2l+1)\eta}\right], \qquad (26)$$

where γ_E is the Euler–Mascheroni constant, $H_n=\sum_{i=1}^n\frac{1}{i}$ is the harmonic number and $\mathrm{Ei}(y)$ is defined as the integral of e^x/x from y to ∞. Notice also that when $k+1$ is divisible by 4 the last term in the sum over l has a spurious pole. The pole in the first term of the last line is cancelled by a zero from a Gamma function.

[3] Note that the expression is finite despite the negative argument of the hypergeometric function as k is assumed to be odd.

Large-k limit The integral (25) can also be exactly evaluated when $k\to\infty$. In order to take the large-k limit, we rescale the integration variable r in (25) by a factor of $k/2$. Recalling the definition of η and using the asymptotic behaviour of the Bessel functions given in (A.2), the integral can easily be performed. It yields

$$\langle W\rangle_{\text{1-loop}} = \langle W\rangle_{\text{1-loop,tad}} \qquad (27)$$
$$\overset{T,k\to\infty}{\simeq} -\frac{T\exp\left[\frac{\eta T}{x_3}\right]}{x_3}\frac{\lambda}{8\pi^2 k}\frac{\sin^2\chi}{\cos^3\chi}\left(\frac{\pi}{2}-\chi-\frac{1}{2}\sin 2\chi\right).$$

Particle-interface potential The expectation value of the Wilson loop is related to the particle-interface potential as

$$\langle W(x_3)\rangle \cong \exp(-T\,V(x_3)), \qquad (28)$$

for $T\to\infty$. At tree level, we therefore have from (11)

$$V_{\text{tree}}(x_3) = -\frac{k-1}{2x_3}\sin\chi, \qquad (29)$$

which agrees with [15]. At one-loop level, however, we expect

$$\langle W(x_3)\rangle_{\text{1-loop}} \cong -T\,V_{\text{1-loop}}(x_3)\exp(-T\,V_{\text{tree}}(x_3)), \qquad (30)$$

such that we can read off the one-loop correction to the potential $V_{\text{1-loop}}(x_3)$ from the Wilson loop $\langle W(x_3)\rangle_{\text{1-loop}}$.

From the vanishing lollipop diagram (15) and the tadpole diagram (24), we then find the following contribution to the potential:

$$V_{\text{1-loop}}(x_3) = V_{\text{1-loop,tad}}(x_3) = V_{\text{tree}}(x_3)\frac{\lambda}{2\pi^2}\frac{\sin\chi}{k-1}\left(\frac{\pi}{4}-A\right). \qquad (31)$$

We notice that there is a point of enhanced symmetry for $\chi=0$ [15]. At this point, the particle-interface potential vanishes and correspondingly the expectation value of the Wilson line is equal to N. The small $\chi=0$ expansion of (31) reads

$$V_{\text{1-loop}}(x_3) = -\frac{\lambda}{2\pi^2}\frac{\chi^2}{x_3}\left[\frac{\pi}{8}\frac{k+2}{k}+\frac{\chi}{k+1}+O(\chi^2)\right]. \qquad (32)$$

The angle χ has some resemblance with the angle of the cusped Wilson loop in pure $\mathcal{N}=4$ SYM theory, for which the small angle expansion could be used to define a so-called Bremsstrahlung function related to the energy emitted by a moving quark [18,19]. It would be interesting to further pursue this line of thought.

4. Comparison to string theory

In the string-theory language, following the idea of [20–22], the expectation value of the Wilson loop can be found in a semi-classical limit, i.e. $N\to\infty$ followed by $\lambda\to\infty$, by evaluating the action of a classical string for which the worldsheet extends from the Wilson line in the boundary of AdS_5 to the D5 brane in the interior and attaches to the D5 brane in such a way that the general D-brane boundary conditions are fulfilled. For this computation, which was done in [15], the exact nature of the D5 brane embedding is important. Let us write the metric of $AdS_5\times S^5$ as

$$\mathrm{d}s^2=\frac{1}{y^2}\left(\mathrm{d}y^2+\mathrm{d}x^\mu\,\mathrm{d}x^\nu\eta_{\mu\nu}\right)+\mathrm{d}\psi^2+\sin^2\psi\,\mathrm{d}\Omega_2^2+\cos^2\psi\,\mathrm{d}\tilde{\Omega}_2^2, \qquad (33)$$

where $x_\mu=(x_0,x_1,x_2)$, the boundary of AdS_5 is located at $y=0$ and

$$\mathrm{d}\Omega_2^2=\mathrm{d}\phi^2+\sin\phi^2\,\mathrm{d}\theta^2, \qquad \mathrm{d}\tilde{\Omega}_2^2=\mathrm{d}\tilde{\phi}^2+\sin\tilde{\phi}^2\,\mathrm{d}\tilde{\theta}^2. \qquad (34)$$

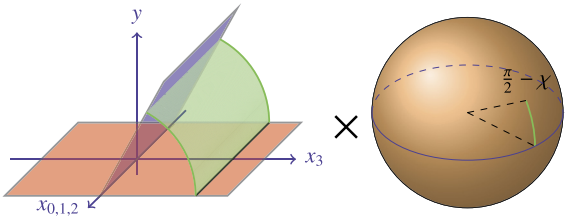

Fig. 2. The minimal surface corresponding to the Wilson loop. In the AdS_5 factor, the minimal surface (green) stretches from the Wilson loop (black) on the boundary (red) to the D5 brane (blue). In the S^5 factor, it is one-dimensional and stretches from the S^2 wrapped by the D5-brane (blue) to the latitude $\frac{\pi}{2} - \chi$ along constant longitude. (For interpretation of the references to colour in this figure legend, the reader is referred to the web version of this article.)

Furthermore, we assume that the background gauge field $\mathcal{F}$ has a flux on the untilded sphere, i.e.

$$\mathcal{F} \sim k \sin\theta \, \mathrm{d}\theta \, \mathrm{d}\phi \,. \tag{35}$$

Then the world volume coordinates of the probe D5 brane are $(x_0, x_1, x_2, y, \theta, \phi)$ and its $AdS_4 \times S^2$ embedding in $AdS_5 \times S^5$ is described by $\tilde{\theta}, \tilde{\phi}$ constant, $\psi = \frac{\pi}{2}$, and

$$y = \frac{\pi k}{\sqrt{\lambda}} x_3 \,. \tag{36}$$

In other words, the AdS_4 part of the D5 brane is tilted with respect to the AdS_5 boundary. For the AdS_4 part of the D5 brane, the correct boundary conditions for the string equations of motion are of Neumann type along the brane and of Dirichlet type transverse to the brane, meaning that the string must be perpendicular to the brane at the point of attachment. This boundary-value problem is of the same type as for the classical pointlike string considered in [12], which is of relevance for the string-theory evaluation of one-point functions in the same defect set-up. Let us parametrise the worldsheet using coordinates $(\tau = t, \sigma)$ with $t \in [-\infty, +\infty]$ and $\sigma \in [0, \sigma_1]$, where $\sigma = 0$ corresponds to the end of the string which is attached to the AdS_5 boundary and σ_1 corresponds to the end of the string which is attached to the D5 brane in the interior of $AdS_5 \times S^5$. The boundary conditions pertaining to the S^5 part of the background geometry then read [15]:

$$\psi = \begin{cases} \chi & \text{for} \quad y = y(\sigma = 0) = 0 \,, \\ \frac{\pi}{2} & \text{for} \quad y = y(\sigma = \sigma_1) \,. \end{cases} \tag{37}$$

The solution of the classical string equations of motion with the above described boundary conditions can be uniquely determined and the corresponding classical action evaluated [15]. We illustrate this in Fig. 2. As usual in the string-theory evaluation of Wilson loops, the integral involved in the evaluation of the action has to be cut-off at a distance ϵ from the boundary of AdS and the divergent $\frac{1}{\epsilon}$-piece removed before the result can be compared to a field-theory computation [22]. The authors of [15] found the particle-interface potential in closed form in the semi-classical limit $N \to \infty$ followed by $\lambda \to \infty$ but suggested to consider the further double-scaling limit

$$\lambda \to \infty, \qquad k \to \infty, \qquad \frac{\lambda}{k^2} \quad \text{fixed}, \tag{38}$$

while keeping $k \ll N$. In this limit, the particle-interface potential reduces to [15]

$$V = V_{\text{tree}} \left[1 + \frac{\lambda}{4\pi^2 k^2} \frac{\sin\chi}{\cos^3\chi} \left(\frac{\pi}{2} - \chi - \frac{1}{2} \sin 2\chi \right) + \mathcal{O}\left(\frac{\lambda^2}{k^4} \right) \right] . \tag{39}$$

Taking the double-scaling limit of our gauge-theory result obtained via (27), we obtain perfect agreement with (39).

The double-scaling limit considered here is very reminiscent of the BMN limit, invented in connection with the study of the spectral problem of $\mathcal{N} = 4$ SYM theory, where another quantum number, J, with the interpretation of an angular momentum was sent to infinity at the same time as λ while the ratio λ / J^2 was kept fixed [23]. In the case of the BMN limit, it eventually turned out that starting at four-loop order the perturbative expansion of the gauge-theory anomalous dimensions did not any longer organise itself into a power series expansion in λ / J^2 [24–26]. Nevertheless, the study of the BMN limit acted as a catalyst for the exploration of the integrability structure of the AdS/CFT correspondence. Whether the gauge-theory observables of the defect set-up will continue to be well defined in the limit (38) at higher loop orders is an open question which deserves further investigation. In any case, one could hope that the double-scaling limit (38) would be the catalyst for revealing the integrability structure of the AdS/dCFT set-up.

5. Conclusions & outlook

In this letter, we have initiated the study of quantum corrections to non-local observables in a class of dCFTs with vevs, derived within the AdS/CFT set-up from $\mathcal{N} = 4$ SYM theory using the duality with certain probe-brane systems carrying background gauge field flux. Concretely, we have calculated the planar one-loop expectation value of an infinite straight Wilson line parallel to the defect, which allowed us to infer the one-loop correction to the particle-interface potential in the dCFT.

Invoking the double-scaling limit described in the previous section, we have compared our result to the string-theory predictions of [15] and found perfect agreement. Considering the rather complicated structure of our result (27), the match we obtain is highly nontrivial. This result is furthermore in line with the results for one-point functions where the comparison of results between gauge and string theory likewise led to agreement [14,16]. Together, the two results thus provide a strong test of the gauge-gravity duality in the case where both conformal symmetry and supersymmetry are partially broken.

An extension of our results to finite N and to two-loop order would be interesting and should in principle be doable, but it is rather technical and beyond the scope of the present publication. It would likewise be interesting to generalise our one-loop analysis to more complicated Wilson loops. One example could be cusped Wilson lines, which have been extensively studied in $\mathcal{N} = 4$ SYM theory where they yield among others the cusp anomalous dimension. A cusped Wilson line would in the present set-up imply the introduction of further angles in addition to the angle of the cusp: the angles specifying the orientation of the cusp relative to the defect. Moreover, polygonal Wilson loops and their possible relation to scattering amplitudes in the dCFT might be worth exploring along the line of [1,27,28]. In particular, the fate of the Yangian symmetry in the presence of a defect would be interesting to investigate for polygonal [29–33] as well as for smooth Wilson loops [34].

Given that integrability has made its appearance in the study of one-point functions in the dCFT under consideration [11–13], it would be interesting to examine if integrability-based methods such as the quantum spectral curve could be applied in the calculation of certain Wilson loops as described for $\mathcal{N} = 4$ in [35,36]. Finally, it would be interesting to investigate to which extent localisation methods, which allow the exact evaluation of a sub-class of Wilson loops in $\mathcal{N} = 4$ SYM theory (see e.g. [37]), can be applied in the defect set-up.

Acknowledgements

We are grateful to S. Caron-Huot, R. Janik, G. Semenoff and K. Zarembo for very helpful discussions. M.d.L., C.K. and M.W. acknowledge partial support by FNU through grants number DFF-1323-00082 and DFF-4002-00037. A.C.I. and, in parts, M.W. were supported by the ERC Advanced Grant 291092.

Appendix A. Bessel functions

We use the following properties of Bessel functions, see for instance [38]:

$$\begin{aligned} z\, I_\nu(z) &= 2\nu\, (I_{\nu+1}(z) - I_{\nu-1}(z))\,, \\ 2\, I'_\nu(z) &= I_{\nu+1}(z) + I_{\nu-1}(z)\,. \end{aligned} \tag{A.1}$$

Their asymptotic behaviour for $\nu \to \infty$ is

$$\begin{aligned} I_\nu(\nu z) &\sim \frac{\mathrm{e}^{\nu\xi}}{\zeta\sqrt{2\pi\nu}}\left[1 + \frac{1}{\nu}\left(\frac{3}{24\zeta} - \frac{5}{24\zeta^3}\right) + \mathcal{O}(\nu^{-2})\right], \\ K_\nu(\nu z) &\sim \frac{\pi\, \mathrm{e}^{-\nu\xi}}{\zeta\sqrt{2\pi\nu}}\left[1 - \frac{1}{\nu}\left(\frac{3}{24\zeta} - \frac{5}{24\zeta^3}\right) + \mathcal{O}(\nu^{-2})\right], \\ I'_\nu(\nu z) &\sim \frac{\mathrm{e}^{\nu\xi}\,\zeta}{z\sqrt{2\pi\nu}}\left[1 - \frac{1}{\nu}\left(\frac{9}{24\zeta} - \frac{7}{24\zeta^3}\right) + \mathcal{O}(\nu^{-2})\right], \end{aligned} \tag{A.2}$$

where $\zeta = (1+z^2)^{1/4}$ and $\xi = \zeta^2 + \log\frac{z}{1+\zeta^2}$.

References

[1] L.F. Alday, J.M. Maldacena, Gluon scattering amplitudes at strong coupling, J. High Energy Phys. 06 (2007) 064, arXiv:0705.0303 [hep-th].
[2] K.G. Wilson, Confinement of quarks, Phys. Rev. D 10 (1974) 2445–2459.
[3] A. Karch, L. Randall, Open and closed string interpretation of SUSY CFT's on branes with boundaries, J. High Energy Phys. 06 (2001) 063, arXiv:hep-th/0105132.
[4] W. Nahm, A simple formalism for the BPS monopole, Phys. Lett. B 90 (1980) 413–414.
[5] D.-E. Diaconescu, D-branes, monopoles and Nahm equations, Nucl. Phys. B 503 (1997) 220–238, arXiv:hep-th/9608163.
[6] A. Giveon, D. Kutasov, Brane dynamics and gauge theory, Rev. Mod. Phys. 71 (1999) 983–1084, arXiv:hep-th/9802067.
[7] N.R. Constable, R.C. Myers, O. Tafjord, The noncommutative bion core, Phys. Rev. D 61 (2000) 106009, arXiv:hep-th/9911136.
[8] J.L. Cardy, Conformal invariance and surface critical behavior, Nucl. Phys. B 240 (1984) 514–532.
[9] K. Nagasaki, S. Yamaguchi, Expectation values of chiral primary operators in holographic interface CFT, Phys. Rev. D 86 (2012) 086004, arXiv:1205.1674 [hep-th].
[10] C. Kristjansen, G.W. Semenoff, D. Young, Chiral primary one-point functions in the D3-D7 defect conformal field theory, J. High Energy Phys. 01 (2013) 117, arXiv:1210.7015 [hep-th].
[11] M. de Leeuw, C. Kristjansen, K. Zarembo, One-point functions in defect CFT and integrability, J. High Energy Phys. 08 (2015) 098, arXiv:1506.06958 [hep-th].
[12] I. Buhl-Mortensen, M. de Leeuw, C. Kristjansen, K. Zarembo, One-point functions in AdS/dCFT from matrix product states, J. High Energy Phys. 02 (2016) 052, arXiv:1512.02532 [hep-th].
[13] M. de Leeuw, C. Kristjansen, S. Mori, AdS/dCFT one-point functions of the SU(3) sector, Phys. Lett. B 763 (2016) 197–202, arXiv:1607.03123 [hep-th].
[14] I. Buhl-Mortensen, M. de Leeuw, A.C. Ipsen, C. Kristjansen, M. Wilhelm, One-loop one-point functions in gauge-gravity dualities with defects, Phys. Rev. Lett. 117 (23) (2016) 231603, arXiv:1606.01886 [hep-th].
[15] K. Nagasaki, H. Tanida, S. Yamaguchi, Holographic interface-particle potential, J. High Energy Phys. 01 (2012) 139, arXiv:1109.1927 [hep-th].
[16] I. Buhl-Mortensen, M. de Leeuw, A.C. Ipsen, C. Kristjansen, M. Wilhelm, A quantum check of AdS/dCFT, J. High Energy Phys. 01 (2017) 098, arXiv:1611.04603 [hep-th].
[17] H. Liu, A.A. Tseytlin, On four point functions in the CFT / AdS correspondence, Phys. Rev. D 59 (1999) 086002, arXiv:hep-th/9807097.
[18] D. Correa, J. Henn, J. Maldacena, A. Sever, An exact formula for the radiation of a moving quark in $\mathcal{N}=4$ super Yang Mills, J. High Energy Phys. 06 (2012) 048, arXiv:1202.4455 [hep-th].
[19] B. Fiol, B. Garolera, A. Lewkowycz, Exact results for static and radiative fields of a quark in $\mathcal{N}=4$ super Yang–Mills, J. High Energy Phys. 05 (2012) 093, arXiv:1202.5292 [hep-th].
[20] S.-J. Rey, J.-T. Yee, Macroscopic strings as heavy quarks in large N gauge theory and anti-de Sitter supergravity, Eur. Phys. J. C 22 (2001) 379–394, arXiv:hep-th/9803001.
[21] J.M. Maldacena, Wilson loops in large N field theories, Phys. Rev. Lett. 80 (1998) 4859–4862, arXiv:hep-th/9803002.
[22] N. Drukker, D.J. Gross, H. Ooguri, Wilson loops and minimal surfaces, Phys. Rev. D 60 (1999) 125006, arXiv:hep-th/9904191.
[23] D.E. Berenstein, J.M. Maldacena, H.S. Nastase, Strings in flat space and pp waves from $\mathcal{N}=4$ superYang–Mills, J. High Energy Phys. 04 (2002) 013, arXiv:hep-th/0202021.
[24] N. Beisert, B. Eden, M. Staudacher, Transcendentality and crossing, J. Stat. Mech. 0701 (2007) P01021, arXiv:hep-th/0610251.
[25] Z. Bern, M. Czakon, L.J. Dixon, D.A. Kosower, V.A. Smirnov, The four-loop planar amplitude and cusp anomalous dimension in maximally supersymmetric Yang–Mills theory, Phys. Rev. D 75 (2007) 085010, arXiv:hep-th/0610248.
[26] F. Cachazo, M. Spradlin, A. Volovich, Four-loop cusp anomalous dimension from obstructions, Phys. Rev. D 75 (2007) 105011, arXiv:hep-th/0612309.
[27] A. Brandhuber, P. Heslop, G. Travaglini, MHV amplitudes in $\mathcal{N}=4$ super Yang–Mills and Wilson loops, Nucl. Phys. B 794 (2008) 231–243, arXiv:0707.1153 [hep-th].
[28] J.M. Drummond, J. Henn, G.P. Korchemsky, E. Sokatchev, On planar gluon amplitudes/Wilson loops duality, Nucl. Phys. B 795 (2008) 52–68, arXiv:0709.2368 [hep-th].
[29] J.M. Drummond, J. Henn, G.P. Korchemsky, E. Sokatchev, Dual superconformal symmetry of scattering amplitudes in $\mathcal{N}=4$ super-Yang–Mills theory, Nucl. Phys. B 828 (2010) 317–374, arXiv:0807.1095 [hep-th].
[30] J.M. Drummond, J.M. Henn, J. Plefka, Yangian symmetry of scattering amplitudes in $\mathcal{N}=4$ super Yang–Mills theory, J. High Energy Phys. 05 (2009) 046, arXiv:0902.2987 [hep-th].
[31] A. Sever, P. Vieira, Symmetries of the $\mathcal{N}=4$ SYM S-matrix, arXiv:0908.2437 [hep-th].
[32] N. Arkani-Hamed, J.L. Bourjaily, F. Cachazo, S. Caron-Huot, J. Trnka, The all-loop integrand for scattering amplitudes in planar $\mathcal{N}=4$ SYM, J. High Energy Phys. 01 (2011) 041, arXiv:1008.2958 [hep-th].
[33] N. Beisert, J. Henn, T. McLoughlin, J. Plefka, One-loop superconformal and Yangian symmetries of scattering amplitudes in $\mathcal{N}=4$ super Yang–Mills, J. High Energy Phys. 04 (2010) 085, arXiv:1002.1733 [hep-th].
[34] D. Müller, H. Münkler, J. Plefka, J. Pollok, K. Zarembo, Yangian symmetry of smooth Wilson loops in $\mathcal{N}=4$ super Yang–Mills theory, J. High Energy Phys. 11 (2013) 081, arXiv:1309.1676 [hep-th].
[35] N. Gromov, F. Levkovich-Maslyuk, Quantum spectral curve for a cusped Wilson line in $\mathcal{N}=4$ SYM, J. High Energy Phys. 04 (2016) 134, arXiv:1510.02098 [hep-th].
[36] N. Gromov, F. Levkovich-Maslyuk, Quark–anti-quark potential in $\mathcal{N}=4$ SYM, J. High Energy Phys. 12 (2016) 122, arXiv:1601.05679 [hep-th].
[37] K. Zarembo, Localization and AdS/CFT correspondence, arXiv:1608.02963 [hep-th].
[38] NIST, Digital library of mathematical functions, http://dlmf.nist.gov/, 1999.